Hydrobiologia (2015) 751:55–72
DOI 10.1007/s10750-014-2171-3

PRIMARY RESEARCH PAPER

Phenotypical variation in *Leucocytherella sinensis* Huang, 1982 (Ostracoda): a new proxy for palaeosalinity in Tibetan lakes

Sascha Fürstenberg · Peter Frenzel · Ping Peng · Karoline Henkel · Claudia Wrozyna

Received: 4 August 2014 / Revised: 29 November 2014 / Accepted: 30 December 2014 / Published online: 23 January 2015

Abstract *Leucocytherella sinensis*, a ubiquitous and the most abundant ostracod endemic to the Tibetan Plateau, can account for >98% of the ostracod association. These low-diversity associations are hard to interpret using community palaeoecology alone, but environmentally driven phenotypic variation may provide clues to palaeoenvironmental factors. *L. sinensis* displays several morphological forms, characterised by different tubercle formation on their valves. These morphological forms were described as diverse species. We present a taxonomical revision and a first description of the soft parts of *L. sinensis*. We also redescribe the genus and confirm its assignment to the subfamily Limnocytherinae Klie, 1938. Analysis of *L. sinensis* associations from surface sediments of 12 Tibetan lakes shows a connection between tubercle formation and specific conductivity (SC) of the ambient water with lower tubercle number at higher salinity. Tubercles are less common in low SC populations and highest within the beta-oligohaline range. However, high Ca^{2+} concentrations suggest a combined effect of salinity and Ca^{2+} ion concentration on tubercle formation. The phenomenon of tubercle formation can be used to trace salinity changes recorded by fossil *L. sinensis* valves from Tibetan Holocene lake sediments.

Keywords Central Asia · Limnocytheridae · Taxonomy · Morphology · Water chemistry · (Palaeo)salinity

Handling editor: Jasmine Saros

S. Fürstenberg (✉) · P. Frenzel
Institute of Geosciences, Friedrich Schiller University Jena, Burgweg 11, 07749 Jena, Germany
e-mail: sascha.fuerstenberg@gmail.com

P. Peng
Institute of Tibetan Plateau Research, Chinese Academy of Sciences, No. 16, Lincui Road, Chaoyang District, Beijing 100101, People's Republic of China

K. Henkel
Institute of Geography, Friedrich Schiller University Jena, Löbdergraben 32, 07743 Jena, Germany

C. Wrozyna
Institute of Earth Sciences, Karl Franzens University Graz, Heinrichstraße 26, 8010 Graz, Austria

Introduction

Ostracods are bivalved microcrustaceans that occur in a variety of aquatic habitats. Their valves, which consist of low-Mg calcite, are easily and abundantly preserved in sediments. Thus, ostracods became popular indicator organisms in palaeolimnology. They record plenty of information about palaeoenvironmental conditions, which can be reconstructed, for example, by population ecology (Boomer et al. 2003; Mischke et al., 2007; Engel et al., 2013), geochemistry (Chivas et al., 1986; Mischke et al., 2010; Börner et al., 2013) or morphological variability (Yin et al., 1999; Uffenorde & Radtke, 2008; Frenzel et al., 2011).

More than half of the lakes on the southern Tibetan Plateau (TP) are oligohaline or highly saline. Since changes in the salinity of endorheic lakes are regarded as reflecting changes in precipitation/evaporation ratios, ostracods can provide useful information about these changes through varying species associations. Another key to tracking changes in salinity can be phenotypical variations, as documented for *Cyprideis torosa* (Hartmann, 1964; Keyser & Aladin, 2004; Keyser, 2005; Frenzel et al., 2011, 2012). A rising specific conductivity (SC) leads to a decreased diversity of ostracod assemblages in continental waters (Mischke et al., 2007); however, the interpretation of environmental changes based on association analysis alone is often flawed. A reconstruction of palaeosalinity using the Mg/Ca ratio (Holmes, 1996) is also difficult because it assumes that stable ion proportions occur in the host water as occur in the marine realm (Anadón et al., 2002).

Leucocytherella sinensis is endemic to the TP and is the dominant ostracod species in great and deep lakes in southern Tibet (Wrozyna et al., 2009b; Frenzel et al., 2010). It shows a strong morphological variation in the number of tubercles and spines on their valves that two genera and 12 species have been defined (Wrozyna et al., 2009b). We assume a connection between tubercle formation and water chemistry for *L. sinensis*, as documented for *Cyprideis torosa* (Hartmann, 1964; Keyser & Aladin, 2004; Keyser, 2005; Frenzel et al., 2012). Hence, this paper addresses the following questions:

1. Are the described two genera and 12 species valid taxa?
2. Are size, shape, ornamentation or tubercle formation associated with water chemistry, e.g. SC or Ca^{2+} content?
3. Can this (possible) link between phenotypical variation and SC or Ca^{2+} content in the water be used to reconstruct changes in palaeosalinity in Tibetan lakes?

A taxonomical analysis of this poorly known species was conducted to serve as a basis for answering these questions. The soft parts, hitherto unknown, are described here for the first time.

Materials and methods

The morphological variation in *L. sinensis* was investigated in 21 recent surface samples from 12 different lakes (Fig. 1; Table 1). Where possible, two samples per lake were chosen—one above and one below the thermocline—to allow inclusion of water depth and water temperature in the analysis. SC was measured by the use of a hand-held conductivity probe (WTW multi 350i) in 0.5–1.0 m water depth. Phytal

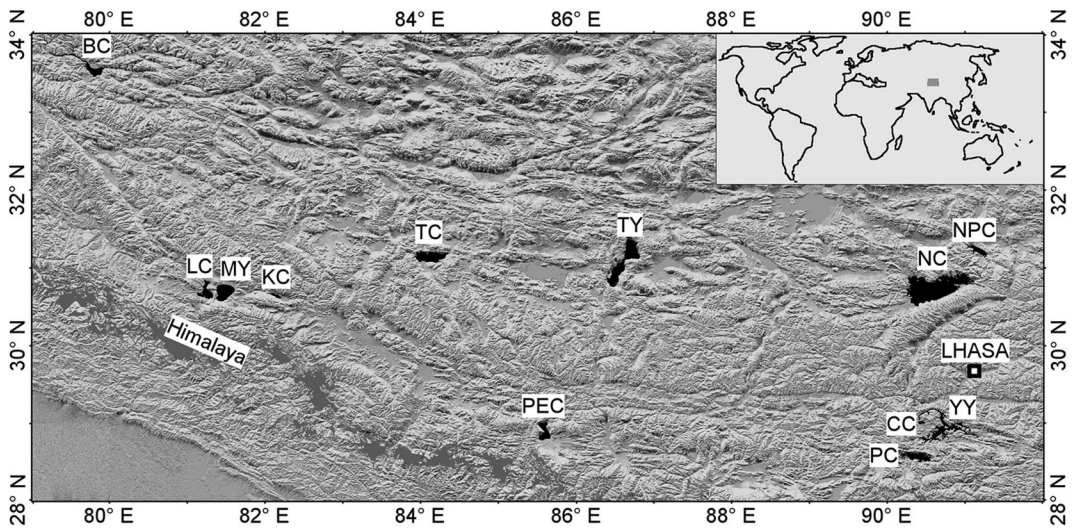

Fig. 1 Morphological map of the Tibetan Autonomous Region and adjacent areas, based on Shuttle Radar Topography Mission data (USGS, 2004) with position of analysed lakes: *BC* Bangong Co, *CC* Chen Co, *KC* Kunggyu Co, *LC* La'ang Co, *MY* Mapam Yumco, *NC* Nam Co, *NPC* Npen Co, *PC* Puma Yumco, *PEC* Peiku Co, *TC* Taro Co, *TY* Tangra Yumco, *YY* Yamdrok Yumco

Table 1 Environmental factors and geochemical data of the analysed samples from the Tibetan Plateau

Sample	Lake (acronym in Fig. 1)	Altitude (a.s.l.)	Water depth (m)	SC (μS/cm)	Ca^{2+} content (mg/l)	pH value	Phytal coverage (%)	Distance to inflow (m)	Substrate
TIP10-7	Tangra Yumco (TY)	4549	0.2	10950	8.2	9.5	50[a]	1	Silt
TIP11-18	Tangra Yumco (TY)	4549	20.4	11880	8.1	9.7	5	590	Silt
TIP11-20	Tangra Yumco (TY)	4549	9.4	11960	8.2	9.6	20	740	Silt
TIP09-35	Npen Co (NPC)	4673	2.0	317	33.5	9.4	5	>2000	Silt (Phytal)
TIP09-26	Npen Co (NPC)	4673	22.0	530	33.5	9.0	0	>2000	Silt
Nam 300805-08	Nam Co (NC)	4718	20.0	1890	9.1	9.3	0[a]	>2000	Fine sand
Nam 300805-10	Nam Co (NC)	4718	30.0	1920	9.1	9.3	0[a]	>2000	Fine sand
TIP08-30 PC	Puma Yumco (PC)	5031	35.0	490	29.4	8.0	0	>2000	Silt
TIP08-32 PC	Puma Yumco (PC)	5031	7.5	492	29.7	9.2	100	>2000	Silt, phytal
TIP08-20	Chen Co (CC)	4438	1.2	1143	70.0	8.5	70	150	Phytal
TIP09-54	Mapam Yumco (MY)	4586	2.3	538	32.5	9.6	30[a]	470	Sand
TIP09-59	Mapam Yumco (MY)	4586	50.0	538	20.8	7.2	0	>2000	Sand
CHN09.j	Mapam Yumco (MY)	4586	0.4	688	33.0[a]	10.4	NaN	NaN	NaN
TIP11-82	Taro Co (TC)	4570	5.7	982	102.7	10.1	75	500	Sand
TIP11-89	Taro Co (TC)	4570	55.8	1017	366.5	9.5	0	>2000	Silt
CHN09.b	Bangong Co (BC)	4353	3.0	896	29.3[b]	8.8	NaN	NaN	Gravel
TIP08-24	Yamdrok Yumco (YY)	4441	12.0	832	35.4	9.0	50[a]	>2000	Algae
TIP08-26	Yamdrok Yumco (YY)	4441	≫12.0	2150	11.1	9.0	0	>2000	Silt
LASS10-8	La'ang Co (LC)	4575	26.0	1460	14.5	NaN	NaN	NaN	Silt
TIP10-KC 03	Kunggyu Co (KC)	4784	15.0	40	16.0	9.2	5	>2000	Sand
CHN09.k	Peiku Co (PEC)	4591	0.2	2540	NaN	9.3	NaN	NaN	Silt

NaN no data collected/available

[a] Data estimated

[b] Data from Bhat et al. (2011)

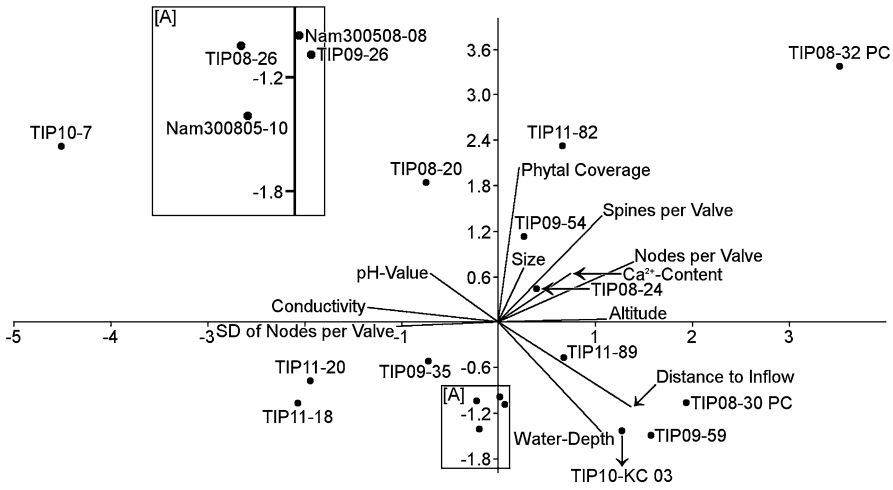

Fig. 2 Principle Components Analysis of environmental factors and morphological features of 17 selected samples; size from different numbers of male valves (Table 2); tubercles per valve, standard deviation of tubercles per valve and spines from 100 valves, both male and female (Table 2); PC1 with eigenvalue: 3.19, variance (%): 28.97; PC2 with eigenvalue: 2.49, variance (%): 22.66

coverage, distance to inflow and the substrate type were assessed by field observations (Table 1).

From every sample, 100 empty valves of both sexes of adult *L. sinensis* were picked randomly and examined using a stereomicroscope. The ratio of male to female valves was nearly 1:1, except for the samples TIP10-7, TIP11-20 and CHN09.b in which this ratio was 0.30, 2.03 and 2.70, respectively.

A photo was taken of every valve using a *Nikon Coolpix S2550* with a fixed focal distance to keep the optical distortion at a minimum. The resulting pictures were measured with *AxioVision LE v. 4.8.2* by *Carl Zeiss MicroImaging GmbH*, with calibration done using a 1-mm scale.

A recent surface sample (TIP09-33) from Npen Co was taken from a depth of 3.7 m within the phytal zone for the ontogenetic studies of *L. sinensis*. This sample was sieved wet into the fractions <200, >200 and >1000 µm. From the fraction of 200–1000 µm, 348 ostracod valves were picked that contained 138 valves clearly assignable to *L. sinensis*. These valves were photographed under a light microscope, and the length and height were measured with *AxioVision LE v. 4.8.2*.

For every valve, the number and position of tubercles or spines were recorded. A thin film of water covering the valve made the counting of tubercles easier through the reflecting light. For the differentiation between tubercles and spines, the valve was tilted around an anterior/posterior line so that the contour of tubercles or spines was visible in dorsal/ventral direction. Additionally, the occurrence or absence of reticulation was recorded. A differentiation between reticulated valves and those without reticulation was also done with a thin film of water which showed just a second before complete evaporation of the reticulation or its absence through the reflecting light. When the reflection displayed a fine meshwork the valve was counted as reticulated and in the case that the reflection showed a single light spot the valve was counted as not reticulated. The final determination of sex was made by the relationship of length to height of the single valves, which was analysed in uncertain cases. Three photos of female and three photos of male right valves were chosen randomly from every sample for the non-metric multidimensional scaling (NMDS) plot of the outline analysis of the valve. Additionally, photos from the right valves of two living *L. sinensis* (♂, TiP08-70NC; ♀, TiP08-27PC), as well as scanned figures of different described species of *Leucocytherella* from Huang et al. (1985) and Pang (1985), were used for the NMDS. Figure 7 on plate 2, displaying a right valve of a female? *Leucocythere dorsotuberosa* in Wrozyna et al. (2009b), was also used for the NMDS. The photo contrast was increased with the image editing software *GIMP 2.6*, and the resulting pictures were converted into two-coloured bitmap files. These were imported into *TPSDig* (Rohlf, 2004) and saved as tps files for use with *Morphomatica* for analysis of the valve outline (Linhart et al., 2006).

The statistical analyses were performed using *Morphomatica* (Linhart et al., 2006), *PAST* (Hammer et al., 2001) and *OpenOffice 3*. The data for the Principle Components Analysis (PCA) were normalised using the following equation: $x_S = (x - m)/\mathrm{sd}$;

Table 2 Size of *L. sinensis* in different lakes on the Tibetan Plateau

Sample	Lake (acronym in Fig. 1)	Male valves					Female valves				
		Mean (μm)	SD (μm)	Minimum (μm)	Maximum (μm)	No. of counted valves	Mean (μm)	SD (μm)	Minimum (μm)	Maximum (μm)	No. of counted valves
TIP10-7	Tangra Yumco (TY)	720	57	606	803	23	678	32	616	778	77
TIP11-18	Tangra Yumco (TY)	689	34	643	784	53	678	31	633	759	47
TIP11-20	Tangra Yumco (TY)	678	34	611	809	67	658	30	610	745	33
TIP09-35	Npen Co (NPC)	721	24	667	767	19	686	37	621	782	81
TIP09-26	Npen Co (NPC)	700	30	614	744	37	642	32	571	707	63
Nam 300805-08	Nam Co (NC)	737	35	649	801	64	683	28	629	729	36
Nam 300805-10	Nam Co (NC)	700	44	622	802	53	674	33	602	737	47
TIP08-30 PC	Puma Yumco (PC)	762	27	692	815	56	718	25	667	773	44
TIP08-32 PC	Puma Yumco (PC)	734	28	657	804	69	670	20	633	710	31
TIP08-20	Chen Co (CC)	771	25	709	808	57	725	27	656	776	43
TIP09-54	Mapam Yumco (MY)	693	31	641	770	44	649	23	607	704	56
TIP09-59	Mapam Yumco (MY)	664	27	603	734	49	637	22	592	683	51
CHN09.j	Mapam Yumco (MY)	756	29	694	809	57	707	34	630	758	43
TIP11-82	Taro Co (TC)	721	23	676	778	57	660	30	598	741	43
TIP11-89	Taro Co (TC)	782	37	671	845	45	732	28	665	791	55
CHN09.b	Bangong Co (BC)	729	26	676	786	73	701	30	631	766	27
TIP08-24	Yamdrok Yumco (YY)	758	50	672	828	47	721	46	606	812	53
TIP08-26	Yamdrok Yumco (YY)	727	28	663	797	59	647	25	602	710	41
LASS10-8	La'ang Co (LC)	707	37	636	811	56	680	23	627	746	44
TIP10-KC 03	Kunggyu Co (KC)	674	31	607	725	37	647	27	539[a]	717	63
CHN09.k	Peiku Co (PEC)	776	43	669	851	59	739	24	690	783	41

[a] Outlier

with x_S is the normalised value; x is the measured value; m is the mean; sd is the standard deviation. The following values were log-transformed for PCA: water depth, distance to inflow, Ca^{2+} content and SC. A two-sample Kolmogorov–Smirnov-test (KS-test) was performed to calculate the difference of tubercle formation between male and female valves. With the test, the distance between the empirical distribution function of two samples (in this case: tubercle formation on male and female valves) is quantified. For SEM pictures, typical morphological variations of *L. sinensis* were picked from different samples and photographed with a *Philips XL 30* scanning electron microscope.

Results

Table 1 shows an overview of the measured environmental parameters. SC of the sampled lakes was between 40 and 11960 µS/cm and nearly constant within the lakes. The only exception is Yamdrok Yumco, which had a SC of 832 µS/cm at 12.0 m water depth and 2150 µS/cm at 12.1 m water depth. The Ca^{2+} content of all sampled lakes was between 5.9 and 366.5 mg/l and showed high variation among the lakes.

The PCA exhibited a variance of 29.0% for PC1 and 22.7% for PC2 (Fig. 2). The Ca^{2+} content showed no correlation with the tubercles ($r^2 = -0.06$), whereas SC reveals a weak to somewhat negative correlation with the development of tubercles ($r^2 = -0.50$).

Valve size

The size of the investigated valves of adult *L. sinensis* ranged between 603 and 851 µm for male specimens and between 571 and 791 µm for female specimens (Table 2; Fig. 3). The female and male individuals were differentiated by the ratio of length to height, where a value of <2.12 indicated a female valve and a value of >2.18 indicated a male valve. Between these two values, both sexes could be represented. In this case, a final decision was made using the shape of the individuals: while female individuals decreased in height posteriorly, male individuals showed dorsal and ventral margin which were nearly parallel.

The measurement of length and height of 138 valves of *L. sinensis* from a Recent surface sample from Npen Co (TiP09-33) revealed ontogenetic

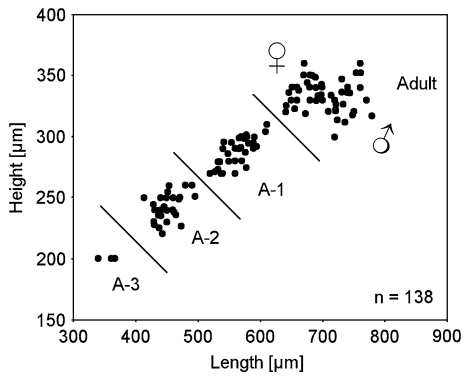

Fig. 4 Ontogenetic stages A-3 until adulthood of *Leucocytherella sinensis*, based on 138 measured male and female valves of a recent surface sample from Npen Co (TIP09-33). In the adult cluster, a separation of females and males is recognisable

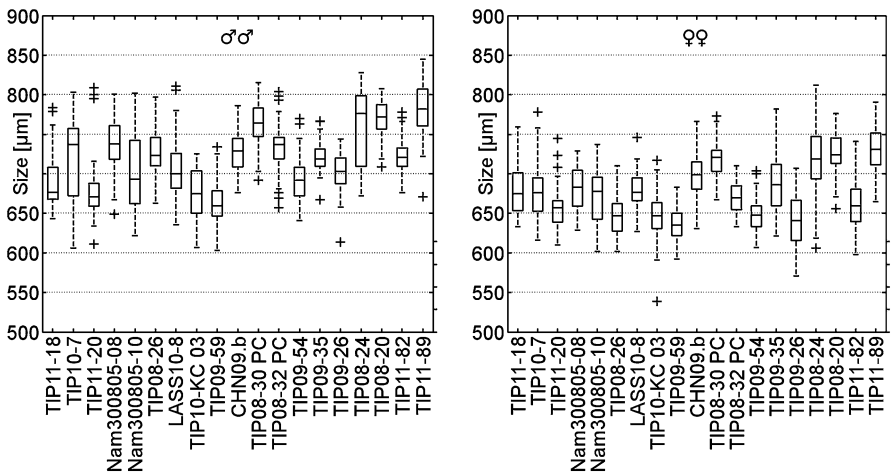

Fig. 3 Boxplots with size of male valves (*left side*) and female valves (*right side*) from *Leucocytherella sinensis*, based on 100 valves per sample with median (*central mark*), 25th/75th percentiles (*edges of each box*), whiskers (extending to most veered values of size not considered as outliers) and outliers (*crosses*)

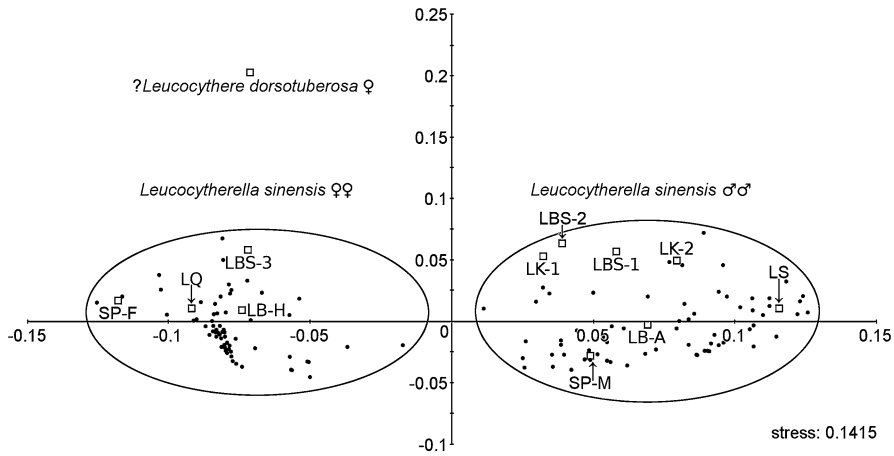

Fig. 5 Non-metric multidimensional scaling of the shape of *Leucocytherella sinensis* and synonymous species with: *SP-F* Soft part-female (TIP08-70NC), *SP-M* soft part-male (TIP08-27PC), *LB-A Leucocytherella biechinata* (Allotype) Huang, 1985, *LB-H Leucocytherella biechinata* (Holotype) Huang, 1985, *LQ Leucocytherella quinquechinata* Huang, 1985, *LS Leucocytherella subtriechinata* Huang, 1985, *LBS-1*, *LBS-2*, *LBS-3 Limnocytherellina bispinosa* Pang, 1985, *LK-1*, *LK-2 Limnocytherellina kunlunensis* Pang, 1985, ?*Leucocythere dorsotuberosa* from Wrozyna et al. (2009a)

growth stages (Fig. 4). The dataset contained instars down to A-3.

Outline analysis

The NMDS plot of the outline analysis showed two main clusters, which represented female valves on the left side and male valves on the right side (Fig. 5). Valves from soft part analysis (SP-F, SP-M) fell inside these clusters, as did most described species of *Leucocytherella* (LB-A, LB-H, LQ, LS, LBS-1, LBS-2, LBS-3, LK-1, LK-2) (Huang et al., 1985; Pang, 1985; Wrozyna et al., 2009b). A shape analysis of a valve from ?*Leucocythere dorsotuberosa*, taken from Wrozyna et al. (2009b), is found outside these two main clusters.

Reticulation

The ratio of valves without reticulation to reticulated valves showed no clear trend in the range of SC from 40 to 2540 µS/cm and the number of valves without reticulation compared to reticulated valves ranged between 0 and 3%. Exceptions, which were significantly different, were the samples TIP10-7, TIP11-18 and TIP11-20 that contained about 15% valves without reticulation. The SC of the lake water for these samples ranged between 10950 and 11960 µS/cm.

Tubercle formation

Tubercles are always developed at the same position on the valve (Fig. 6). A maximum of five tubercles occurs on each valve. A linear Delauney interpolation of tubercle formation on 100 valves per sample plotted against SC and Ca^{2+} content (Fig. 7) showed a pattern in which the maximum number of tubercles occurred at a SC of 530 µS/cm and a Ca^{2+} content of 30 mg/l. With increasing SC or increasing Ca^{2+} ions, the tubercle formation decreased. Below 530 µS/cm, the tubercle formation also decreased. The Mg^{2+} content, when tested against tubercle formation and SC, showed no clear pattern.

The development of spines plotted against SC and Ca^{2+} content (Fig. 8) showed a comparable pattern to that seen for tubercle formation. The greatest numbers of spines were also found at a SC of 530 µS/cm and a Ca^{2+} content of 30 mg/l. However, another peak of spines was observed at ~1000 µS/cm and ~100 mg/l Ca^{2+}. When picking and classifying the adult individuals from the samples, it showed that juvenile individuals tend to have more spines than adult ones. But no quantitative data on this issue were collected.

The two-sample KS-test showed no significant difference between the tubercle formation in female and male valves. The sample with the highest differences in tubercle formation between male and female

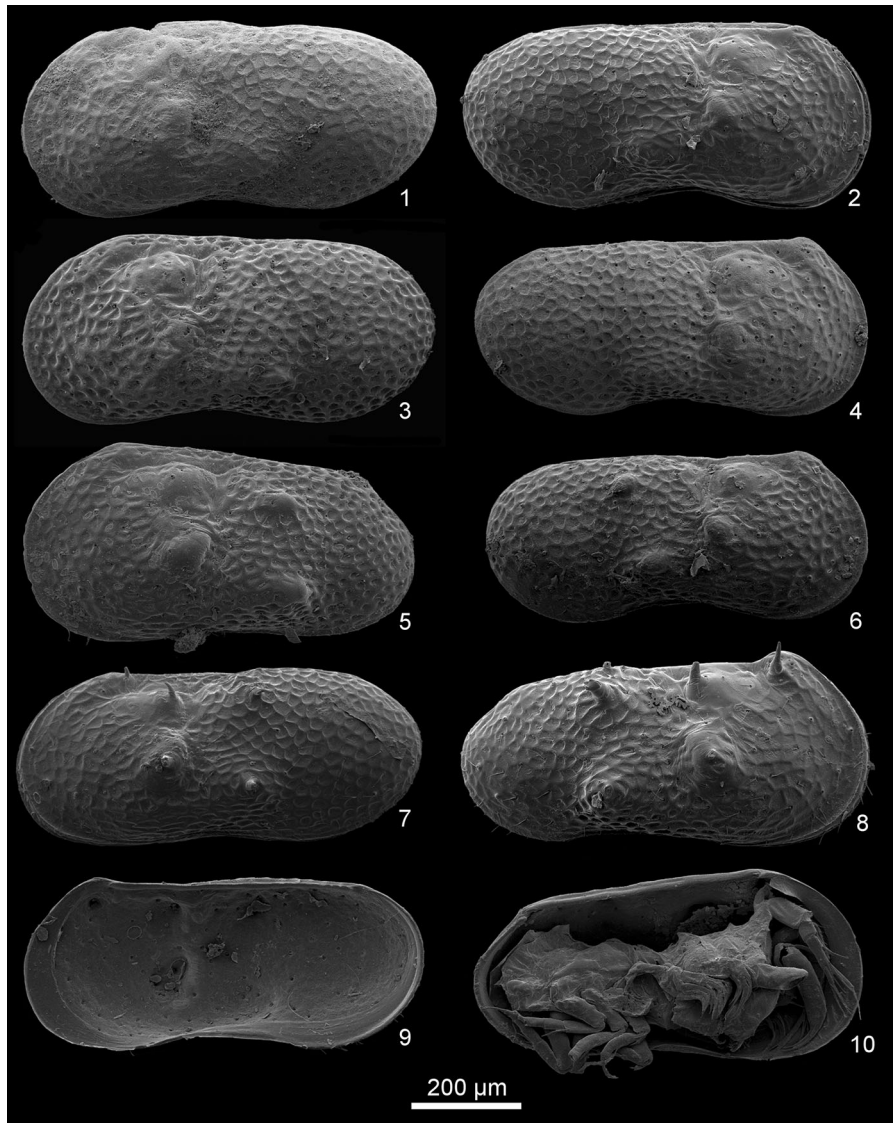

Fig. 6 SEM pictures of adult *Leucocytherella sinensis*: *1* ♂ LV (TIP10-07), *2* ♂ right side of the carapace (Nam300805-08), *3* ♂ LV (TIP08-30 PC), *4* ♂ RV (TIP09-35), *5* ♀ LV (TIP09-54), *6* ♂ RV (TIP09-26), *7* ♂ LV (TIP08-32 PC), *8* ♀ RV (TIP08-32 PC), *9* ♂ RV (TIP08-32 PC), *10* ♀ LV (TIP08-32 PC)

valves was TIP09-26 and it showed the lowest *P* value, with $P = 0.946$.

Discussion

Size

The size of adult male and female *L. sinensis* varies between different lakes (Fig. 3). No pattern in the distribution of size (e.g. habitat or latitude) could be determined. Also, no correlation is noted between size and SC or water depth. A decreasing water depth would lead to a rise in temperature, which aids ostracod growth, for example, as recorded for *Candona rawsoni* by Xia et al. (1997). Salinity also could influence ostracod growth, as shown, for example, for *Limnocythere inopinata* by Yin et al. (1999).

Outline analysis

The outline analysis indicates that the described species of *Leucocytherella* from the TP belong to one species: *L. sinensis*. This assumption is deduced from the occurrence of all analysed samples as well as the shapes of the holotypes and allotypes inside the

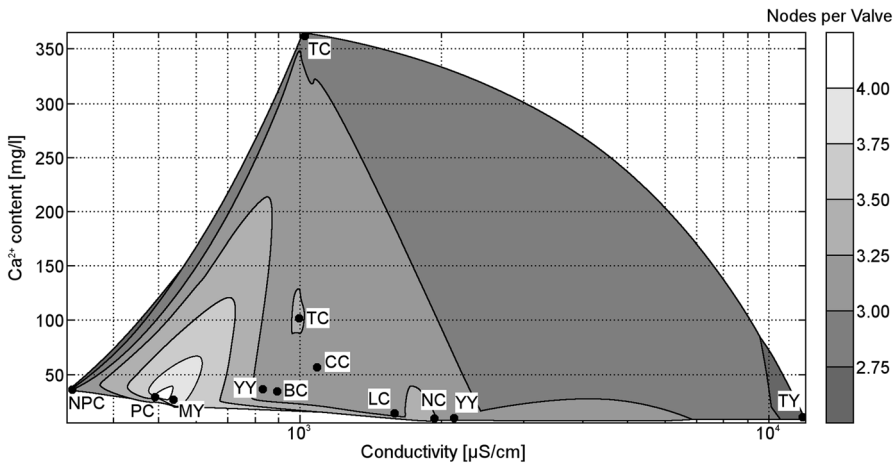

Fig. 7 Tubercle formation per valve as a function of SC and Ca^{2+} content (Table 1) with *black dots* representing the position of analysed lakes: *BC* Bangong Co, *CC* Chen Co, *LC* La'ang Co, *MY* Mapam Yumco, *NC* Nam Co, *NPC* Npen Co, *PC* Puma Yumco, *TC* Taro Co, *TY* Tangra Yumco, *YY* Yamdrok Yumco

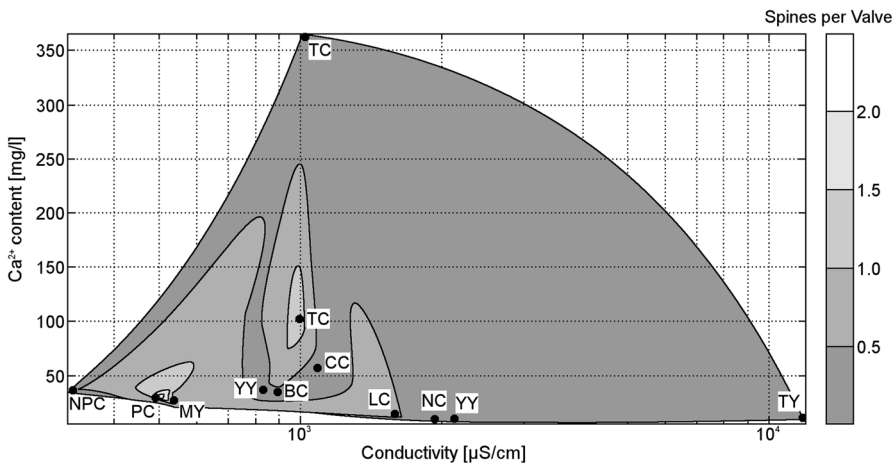

Fig. 8 Spines per valve as a function of SC and Ca^{2+} content (Table 1), with *black dots* representing the position of analysed lakes: *BC* Bangong Co, *CC* Chen Co, *LC* La'ang Co, *MY* Mapam Yumco, *NC* Nam Co, *NPC* Npen Co, *PC* Puma Yumco, *TC* Taro Co, *TY* Tangra Yumco, *YY* Yamdrok Yumco

two main clusters in the NMDS in Fig. 5. The fact that the similar ?*Leucocythere dorsotuberosa* (which, like *L. sinensis*, belongs to the tribe of Danielopol et al. 1989) is clearly outside these two clusters supports this idea. In a different way from *Eucypris virens* in which carapace "shape variability increases significantly when organisms are raised under fluctuating environmental conditions" (Baltanás et al., 2000), the shape of *L. sinensis* seems not to be influenced by any of the considered environmental factors.

Reticulation

The increase of valves without reticulation compared to reticulated valves in localities with higher salinities points to an indication for reconstruction of palaeosalinities. The number of valves without reticulation changes from ~3% between a SC of 0 and 2,500 µS/cm to ~15% at a SC of about 10^4 µS/cm. Hence, reticulation can be used for reconstructing large changes in palaeosalinity (>2500 µS/cm).

Tubercle formation

The phenomenon of tubercle formation in *L. sinensis* depends on salinity and the Ca^{2+} content, whereas the Mg^{2+} content seems to have no influence on the development of tubercles. Therefore, the changes in tubercle formation show a clear trend that enables the reconstruction of palaeosalinity, with the restriction of following confinement: A change in the Ca^{2+} concentration alters the number of tubercles at a given

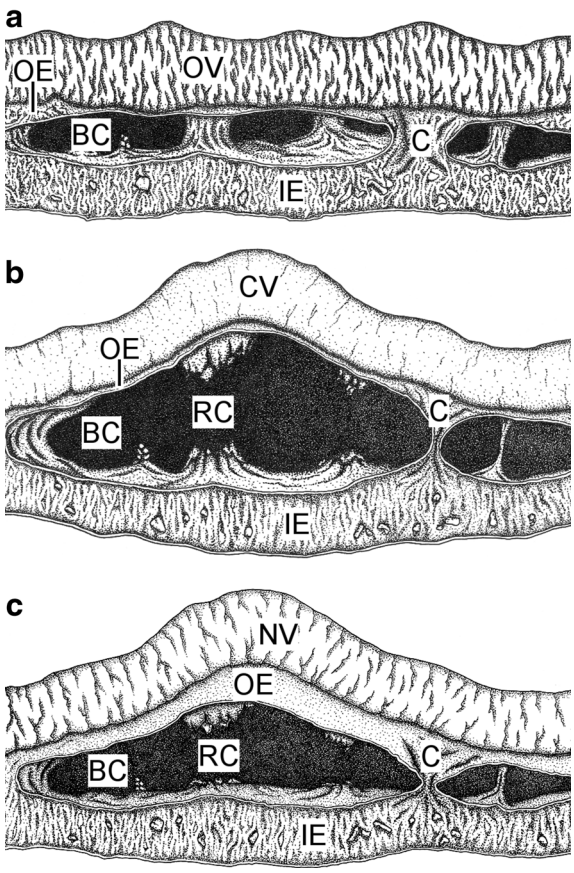

Fig. 9 Schematic illustration of possible process of tubercle formation in *Leucocytherella sinensis* as described for *Cyprideis torosa* (Keyser, 2005) with: **a** individual prior to the moulting; **b** osmotic pressure causing inflow of ambient water and widening of body cavities; separating of valve from body; ongoing inflow of ambient water causing rupture of connections between body cavities while new valve calcifies; **c** calcified new valve representing swelling while osmoregulation leads to a decrease of water inside the individual. *OV* old valve, *OE* outer epidermal cell layer, *BC* body cavity, *C* connection, *IE* inner epidermal cell layer, *RC* ruptured connection, *CV* calcifying valve, *NV* new valve

salinity, but at about 530 µS/cm, no clear conclusion can be made since the number of tubercles decreases in both directions.

Apart from the salinity of the ambient water, Ca^{2+} is also of crucial importance for the occurrence of tubercles. A lack of available Ca^{2+} in the ambient water leads to a failure in muscle and desmosomal activities, which is comparable to a cramp and can cause ruptures of the connections between inner and outer epidermal cell layer (Keyser, 2005). An excess water inflow during moulting of the ostracods may cause the tubercles to swell in the not yet calcified cuticula (Fig. 9). Biomineralisation of these pathological tubercles on the body surface will stabilise and conserve those structures, as is already known from *Cyprideis torosa* (Keyser, 2005; Frenzel et al., 2012), another Cytheracean ostracod which develops tubercles at a salinity lower than 7 psu (Frenzel et al., 2012).

Based on Keyser (1990, 2005), who investigated the phenomenon of tubercle formation in *C. torosa*, Turpen & Angell (1971), and our own observations, the theory for the process of tubercle formation in *L. sinensis* can be described in three successive stages (Fig. 9):

(N–1) SC in the ambient water is lower than in the organism itself. A specific quantity of salt is gained in the body fluid in this hyperosmotic environment through an enrichment of salt absorbed with the food (Aladin & Potts, 1996).

(N–2) During the moulting process, the old valve is separated from the outer epidermal cell layer by body fluid which is "distributed throughout the shell by a kind of weak circulatory system" (Keyser, 2005). In those places where the circulatory system is connected to the system of the body itself the "pressure is applied first and therefore these places are most likely to tear apart" (Keyser, 2005). The osmotic pump of the individual cannot deal with the amount of inflowing liquid and the cavities swell. The resulting increase in volume should define the size of the valve of the next stage (Anderson, 1964; Turpen & Angell, 1971), but the continuous uncontrolled influx of water as well as the lack of Ca^{2+} leads to a rupture of the connections between the inner and the outer epidermal cell layers as well as to a connection of single cavities within the tissue. This causes a blowing up of the outer epidermal cell layer at the same time as the new valve is developing and calcifying. This model is supported by the fact that the reticulation often is

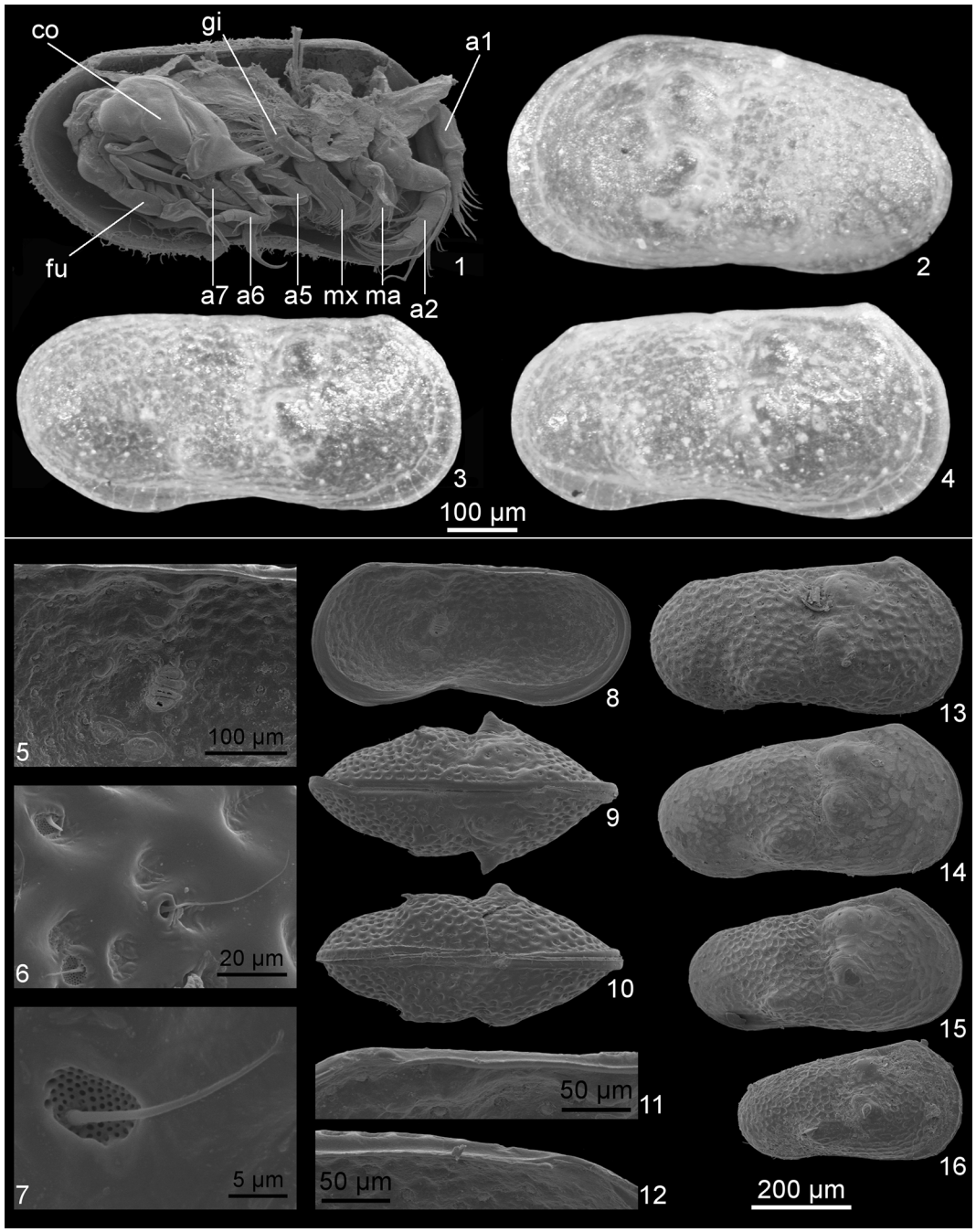

Fig. 10 SEM-pictures and light microscopic images of *Leucocytherella sinensis* with *1* LV, ♂ (from Frenzel et al., 2014) softpart with *a1* first antenna, *a2* second antenna, *ma* mandible, *mx* maxilla, *a5* 5th appendage, *a6* 6th appendage, *a7* 7th appendage, *fu* furca, *co* copulatory organ, *gi* gills; *2* LV, holotype, (NIGP 59545); *3* RV, holotype, (NIGP 59544); *4* RV, holotype, (NIGP 59542); *5* RV internal, ♂, muscle scars; *6* pores; *7* ventral, ♀, sieve pore; *8* RV, internal, ♂; *9* dorsal, ♀; *10* ventral, ♀; *11* RV, internal, ♂, anterior hinge; *12* RV, internal, ♂, posterior hinge; *13* RV, ♀, adult; *14* RV, A-1, *15* RV, A-2; *16* RV, A-3

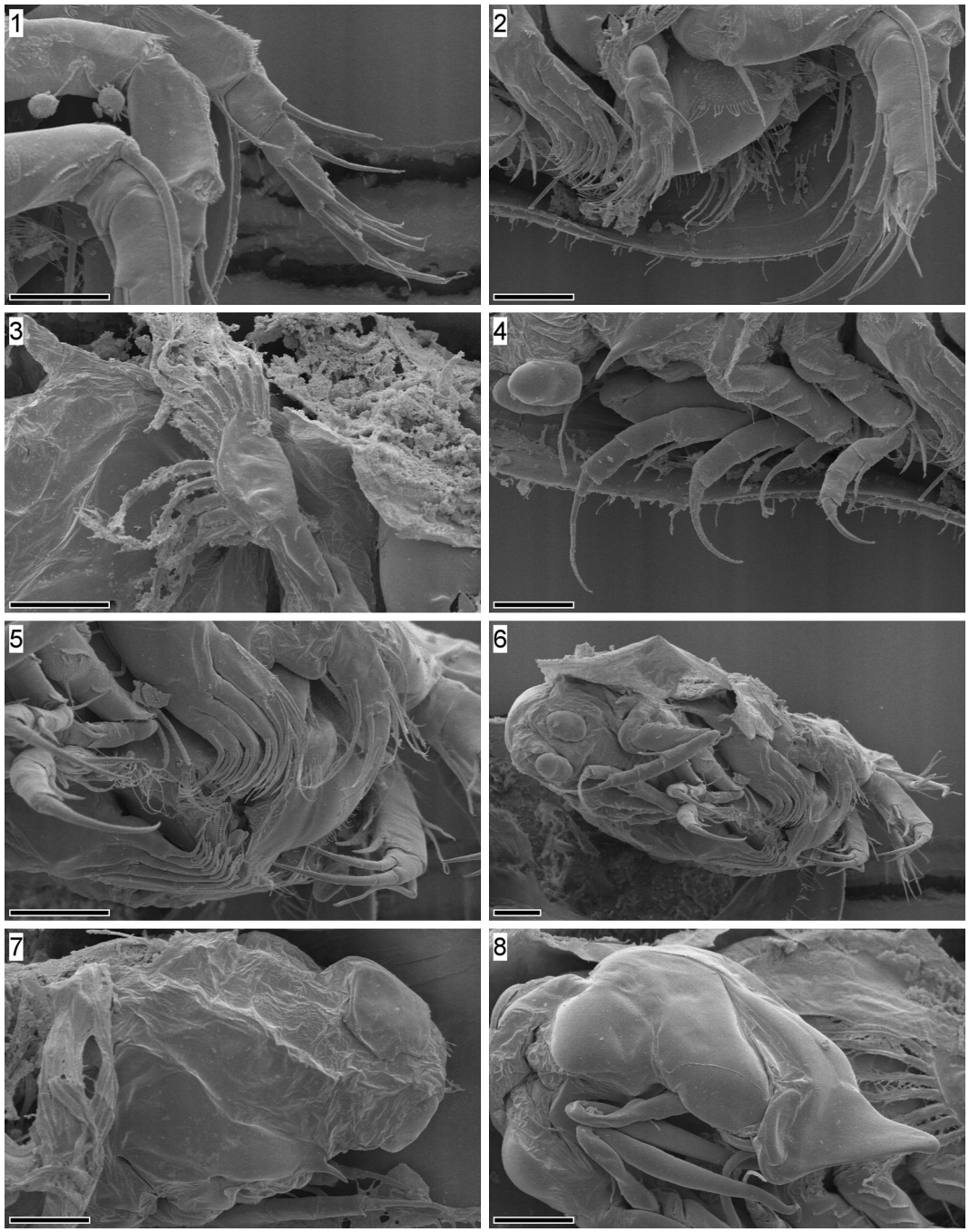

Fig. 11 SEM-pictures with softpart details of *Leucocytherella sinensis* with *1* A-1, antennula, TiP08-71NC; *2* A-1, antenna, mandibula and maxillula, TiP08-71NC; *3* A-1, gills, TiP08-71NC; *4* A-1, walking legs, TiP08-71NC; *5* ♀, mandibula and maxillula, TiP08-70NC; *6* ♀, softparts in ventral view, TiP08-70NC; *7* ♀, copulatory organ, TiP08-70NC; *8* ♂, hemipenis, TiP08-70NC; *scale bar* is 50 µm for all figures

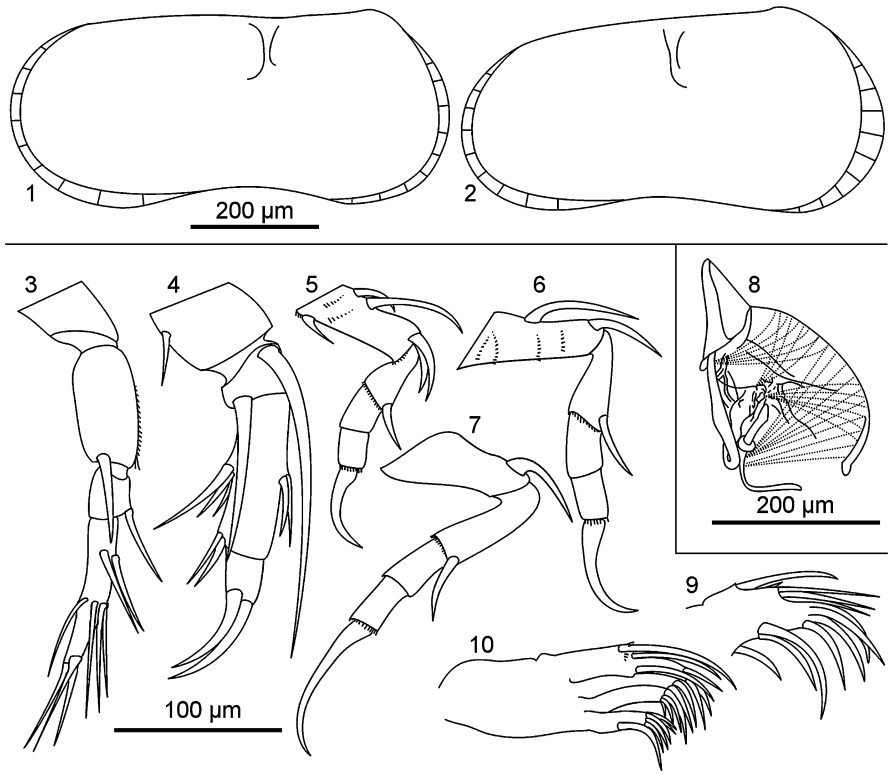

Fig. 12 Schematic illustrations of *Leucocytherella sinensis* with *1* ♂, RV; *2* ♀, RV; *3* ♀, antennula; *4* ♀, antenna; *5* ♀, L5; *6* ♀, L6; *7* ♀, L7; *8* ♂, copulatory organ; *9* ♀, mandibula; *10* ♀, maxillula

stretched or missing on top of the tubercle and that bulges are evident on the rim of the tubercle that develops when it partially collapsed back.

(N–3) After calcification is completed, the surplus liquid is removed from the body and the cavities of the tissue diminish nearly to their original size. The valve that calcified over the swelling has an excrescence, and therefore represents a calcified accident in osmoregulation.

Spines

Spines as well as tubercles point to a lowered salinity, though the variance is too high for use in reconstructing palaeosalinity (Fig. 8). This may be caused by an additional functional role like protection against (micro-) predators, as described for *Diacypris spinosa* (De Deckker & Martens, 2013) (illustrated in De Deckker, 1981) since juvenile individuals show more spines than adult ones.

Conclusion

The occurrence of tubercles is not a taxonomical character but depends on salinity and the concentration of Ca^{2+} ions. If the proportion of Ca^{2+} ions stays constant, trends in salinity can be detected by counting the tubercles on the valves of adult individuals. Based on morphological analysis, it emerges that the 12 species of *Leucocytherella* described from the TP are synonyms of one species: *L. sinensis*.

Taxonomic revision

Leucocytherella sinensis Huang, 1982 (Figs. 6, 10, 11, 12)

v*	1982	*Leucocytherella sinensis* gen. et sp. nov. Huang—Huang et al., p. 341, pl. 12, Figs. 1-8; pl. 13, Figs. 1–7 [type species of *Leucocytherella* Huang, 1982]
v•	1982	*Leucocytherella trinoda* gen. et sp. nov. Huang—Huang et al., p. 342, pl. 14, Figs. 4–18
v•	1982	*Leucocytherella glabra* gen. et sp. nov. Huang & You—Huang et al., p. 342, pl. 16, Figs. 1–10
v•	1982	*Leucocytherella hyalina* gen. et sp. nov. Huang & You—Huang et al., p. 343, pl. 15, Figs. 1–12; pl. 16, Figs. 11–16
•	1985	*Limnocytherellina trispinosa* gen. et sp. nov. Pang—Pang, p. 270–271, pl. 1, Figs. 1–6; pl. 2, Figs. 1–4 [type species of *Limnocytherellina* Pang, 1985]
•	1985	*Limnocytherellina bispinosa* gen. et sp. nov. Pang—Pang, p. 271–272, pl. 1, Figs. 7–14; pl. 3, Figs. 1–10
•	1985	*Limnocytherellina kunlunensis* gen. et sp. nov. Pang—Pang, p. 272, pl. 1, Figs. 15–16; pl. 2, Figs. 5–10
v•	1985	*Leucocytherella biechinata* sp. nov. Huang—Huang et al., p. 374, pl. 3, Figs. 5, 6
v•	1985	*Leucocytherella triechinata* sp. nov. Huang—Huang et al., p. 374, pl. 2, Figs. 6, 7
v•	1985	*Leucocytherella subtriechinata* sp. nov. Huang—Huang et al., p. 374, pl. 3, Figs. 7, 8
v•	1985	*Leucocytherella quadriechinata* sp. nov. Yang—Huang et al., p. 374, pl. 3, Figs. 9, 10
v•	1985	*Leucocytherella quinquechinata* sp. nov. Huang—Huang et al., p. 374, pl. 3, Figs. 11, 12
•	1985	*Limnocytherellina trispinosa* Pang—Pang et al., pl. 1, Figs. 12–21
•	1985	*Limnocytherellina bispinosa* Pang—Pang et al., pl. 2, Figs. 1–9
•	1985	*Limnocytherellina kunlunensis* Pang—Pang et al., pl. 2, Figs. 10–12
•	1991	*Limnocytherellina trispinosa* Pang—Li et al., pl. 1, Figs. 22, 23
•	1997	*Leucocytherella sinensis* Huang—Peng, J., pl. 1, Figs. 13–16
•	1997	*Leucocytherella* cf. *sinensis* Huang—Peng, J., pl. 2, Figs. 1–3
•	1997	*Leucocytherella trinoda* Huang—Peng, J., pl. 2, Fig. 4
v•	2007	*Leucocytherella sinensis* Huang—Hou & Gou, p. 155, pl. 37, Figs. 1–4 [kop. Huang et al., 1982]
•	2007	*Leucocytherella hyalina* Huang & You—Hou & Gou, p. 155, pl. 37, Figs. 5–11 [Fig. 7 kop. Huang et al., 1982], pl. 38, Figs. 1–4
•	2007	*Leucocytherella subtriechinata* Huang—Hou & Gou, p. 155, pl. 38, Figs. 9–12 [Figs. 11 & 12 kop. Huang et al., 1985]
•	2007	*Leucocytherella quinquechinata* Huang—Hou & Gou, p. 156, pl. 38, Figs. 5–8 [Figs. 5 & 6 kop. Huang et al., 1985]
•	2009a	*Leucocytherella sinensis* Huang—Wrozyna et al., p. 8, pl. 3, Figs. 2–16
•	2009b	*Leucocytherella sinensis* Huang—Wrozyna et al., p. 667–668, pl. 1, Figs. 1–6
•	2010	*Leucocytherella sinensis* Huang—Wrozyna et al., Fig. 3, no. 5
•	2010	*Leucocytherella sinensis* f. *typica* Huang—Zhu et al., Fig. 3, no. 9
•	2010	*Leucocytherella sinensis* f. *trinoda* Huang—Zhu et al., Fig. 3, no. 10
•	2012	*Leucocytherella sinensis* Huang—Jochum et al., p. 32, Fig. 1b
•	2013	*Leucocytherella sinensis* Huang—Börner et al., Fig. 1
•	2014	*Leucocytherella sinensis* Huang—Frenzel et al., p. 111
•	2014	*Leucocytherella sinensis* Huang—Yang et al., Fig. 2

Material

Several thousand valves from 12 large lakes on the central and southern TP; this set includes a large number of articulated valves and several hundred carapaces with soft parts.

Dimensions

Length (female): 571–791 μm; (male): 603–851 μm

Height (female): 287–394 μm; (male): 250–390 μm

Holotype

Collection of the Nanjing Institute of Geology and Palaeontology (NIGP), Chinese Academy of Sciences; No. 59541–59550; Age: Pliocene to Holocene; Distribution: Province of Xizang, China; Remarks: The initial description was done on an empty valve, lacking the soft parts.

Length (NIGP: 59542): 696 μm; (NIGP: 59544): 750 μm; (NIGP: 59545): 649 μm
Height (NIGP: 59542): 346 μm; (NIGP: 59544): 330 μm; (NIGP: 59545): 338 μm

Description

Valves of *L. sinensis* show a straight dorsal margin and both ends are evenly rounded in lateral view. The ventral margin is more or less pronounced concave. The dorsal margin is bordered by a distinct angle anteriorly and a much smoother one posteriorly. Males are larger and more expanded posteriorly than females, resulting in parallel ventral and dorsal sides in lateral view of males. The external ornamentation consists of a regular reticulation smoothing to the anterior margin and on distinct tubercles. Tubercles may distort the regular ornamentation. Individuals from beta-mesohaline lakes can show a tendency to smooth valves without reticulation and tubercles. Two weak sulci start in the anterior half of the valve, one of those directly behind the anteriodorsal angle; they vanish before they reach mid-height. In lateral view, the posterior sulcus is the longer one. The valves may bear up to five tubercles in fixed positions (Figs. 6, 10). Two tubercles are situated between the two sulci; two other tubercles lie behind the more posterior sulcus and the fifth tubercle, which is rarely developed, is located close to the anteriodorsal angle. The degree of tubercle formation can vary from weak swellings to prominent tubercles without ornamentation or even to spines on top of the tubercles. Tubercles and spines are hollow.

Both sides of the carapace are parallel in dorsal view while the anterior end is pointed rather than beak-shaped. The posterior end is rounded. The left valve overlaps the right valve anteriorly, followed by a lobe-like extension of the right valve protruding over the left one immediately in front of the anterior tooth of the hinge on the right valve. The right valve overlaps the left valve distinctively posteriorly.

Seen in internal view, the narrow duplicature of the inner lamella runs more or less parallel to the outer margin. It is broadest anteriorly (7.0–7.5% of shell length) and relatively broad ventrally, but lacks a vestibulum. For the right valve, the lophodont hinge shows an anterior tooth followed by a long groove; its anterior part is L-shaped in cross-section and not closed anteriorly. The proximal margin bends upward posteriorly and forms the edge of the valve thus ending the dorsal groove. The hinge of the left valve is characterised by a smooth central bar ending on both sides with a socket. The central muscle scars are arranged in an almost vertical row of four elliptical similar-sized scars. The pair of mandibular scars is situated below and slightly in front of these; a single scar can be seen in the same distance to the dorsal valve margin as the uppermost of the scars in the row but more anteriorly (Fig. 10, no. 5).

The marginal pore channels are simple and straight; nine anterior and posterior. The exterior openings of the normal pore channels are surrounded by a ridge and closed by sieve plates either near to the surface of the shell or deeply counter-sunk into it.

The antennule is similar to those of *Leucocythere mirabilis* described by Danielopol et al. (1989). The antenna differs from *L. mirabilis* in that way that only two terminal setae are present, and no differences are recognisable in the structure of the antenna between males and females. Furthermore, one seta can be found at the very proximal segment, which is not depicted in Danielopol et al. (1989). The fifth to seventh limb are four-segmented walking legs. The fifth limb shows the same structure as given for *L. mirabilis* by Danielopol et al. (1989), except that the apical seta on the second segment is rather short and does not extend over the whole second segment. The sixth limb is very similar to the fifth one but bears only one anterior seta on the first segment as well as it bears only one knee seta. The seventh limb displays one knee seta with half the size of the second segment and one anterior seta on the third segment that slightly reaches over the third segment. The respiratory plate on the first segment of the mandibular palp shows eight rays pointing in the dorsal direction and six rays pointing in the posterior direction. The maxillula bears six setae on the uppermost segment and at least two setae on the penultimate segment. The segment below shows at least four setae and the last segment bears six setae. The hemipenis bears three groups of muscles, which are located in different places inside the labyrinth and one muscle in the ventral part. As stated by Karanovic (2012) in the description for the tribe of Leucocytherini, the copulatory process is spirally shaped.

Interpretation

Tubercles on the valves of *Leucocytherella* cannot be used for determination and classification of different *Leucocytherella* species because their occurrence or absence depends on the salinity and calcium content of the ambient water. In a different way from *Leucocythere*, *Leucocytherella* bears two setae on the antenna, which can be used to discriminate these two genera. The generic name *Limnocytherellina* is a younger synonym of *Leucocytherella* and should be avoided.

Diagnosis of *Leucocytherella*

Different from the genus *Leucocythere*, *Leucocytherella* shows only two setae on the last segment of the antenna. Furthermore the valves of *Leucocytherella* are more elongated than those of *Leucocythere* and the posterior margin is less broad. The lophodont hinge on the right valve shows a tooth in the anterior part which is merging into a long groove. The hinge of the left valve has a socket on each end and smooth central bar in between these two sockets.

Comparisons and systematics

The highest risk of confusion with *L. sinensis* occurs with juvenile *Leucocythere dorsotuberosa*. Different from *L. sinensis*, juvenile *L. dorsotuberosa* show a broader posterioventral margin. For living individuals, the difference between these two species can be found on the antenna, since *L. sinensis* bears only two setae and *L. dorsotuberosa* bears three setae on the terminal segment. *Leucocytherella* displays all the features as they are given for the family of Limnocytheridae Klie, 1938, except for one difference: The antenna of *Leucocytherella* shows only two claws on the terminal segment. We suggest extending the key for the family Leucocytheridae Klie, 1938 as given by Karanovic (2012) to comprise taxa with three or two claws on the terminal segment on the antenna. *Leucocytherella* also displays all the features as given for the subfamily of Limnocytherinae Klie, 1938 by Karanovic (2012). Considering the definition of Leucocytherini by Danielopol et al. (1989), *Leucocytherella* shows all diagnostic features of this tribe except a crenulated hinge bar. The hinge is lophodont, as given for Leucocytherini, but the hinge bar is smooth. The arrangement and expression of the sulci are slightly different from *Leucocythere*. The attribution of *Leucocytherella* to the tribe Leucocytherini is not clear and needs more investigation.

The phenomenon of tubercle formation in *L. sinensis* can be used as a new proxy for palaeosalinity reconstruction in Quaternary sediments from lakes of the TP. Further research can use DNA analysis to confirm the assignment of all species described above to *L. sinensis*. Experiments with living individuals performed under controlled salinity and Ca^{2+} content could also allow the setup of a transfer function that could be used to compute quantitative data for palaeosalinity in Tibetan lakes.

Acknowledgements We thank Steffen Mischke, Franziska Günther, Nicole Börner, Junbo Wang, Liping Zhu, Baoren Huang and Yunxian Gou for providing samples and fruitful discussions. This work is part of the DFG priority program 1372 "TiP: Tibetan Plateau–Formation–Climate–Ecosystems". We also would like to thank the anonymous reviewer who helped to improve the manuscript with constructive criticism.

References

Aladin, N. V. & W. T. W. Potts, 1996. The osmoregulatory capacity of the Ostracoda. Journal of Comparative Physiology B 166: 215–222.

Anadón, P., E. Gliozzi & I. Mazzini, 2002. Paleoenvironmental reconstruction of marginal marine environments from combined paleoecological and geochemical analyses on ostracods. In Holmes, J. A. & A. Chivas (eds), The Ostracoda: Applications in Quaternary Research. Geophysical Monograph 131. American Geophysical Union, Washington, DC: 227–247.

Anderson, F. W., 1964. The law of ostracod growth. Palaeontology 7: 85–104.

Baltanás, A., M. Otero, L. Arqueros, G. Rossetti & V. Rossi, 2000. Ontogenetic changes in the carapace shape of the non-marine ostracod *Eucypris virens* (Jurine). In Horne, D. J. & K. Martens (eds), Evolutionary Biology and Ecology of Ostracoda. Springer, Netherlands: 65–72.

Bhat, F. A., A. R. Yousuf, A. Aftab, J. Arshid, M. D. Mahdi & M. H. Balkhi, 2011. Ecology and biodiversity in Pangong Tso (lake) and its inlet stream in Ladakh, India. International Journal of Biodiversity and Conservation 3: 501–511.

Börner, N., B. De Baere, Q. Yang, K. P. Jochum, P. Frenzel, M. O. Andreae & A. Schwalb, 2013. Ostracod shell chemistry as proxy for paleoenvironmental change. Quaternary International 313–314: 17–37.

Boomer, I., D. J. Horne & I. J. Slipper, 2003. The use of ostracods in palaeoenvironmental studies, or what can you do with an ostracod shell? In Park, L. E. et al. (eds), Bridging the Gap: Trends in the Ostracode Biological and Geological Sciences. The Palaeontological Society, Papers 9. Yale University, New Haven: 153–179.

Chivas, A. R., P. De Deckker & J. M. G. Shelley, 1986. Magnesium and strontium in non-marine ostracod shells as indicators of palaeosalinity and palaeotemperature. Hydrobiologia 143: 135–142.

Danielopol, D. L., K. Martens & L. M. Casale, 1989. Revision of the genus *Leucocythere* KAUFMANN, 1892 (Crustacea, Ostracoda, Limnocytheridae), with description of a new species and two new tribes. Bulletin de l'Institut Royal des Sciences Naturrelles de Belgique=Mededelingen-Koninklijk Belgisch Instituut voor Natuurwetenschappen 59: 63–94.

De Deckker, P., 1981. Taxonomic notes on some Australian ostracods with the description of a new species. Zoologica Scripta 10: 37–55.

De Deckker, P. & K. Martens, 2013. Extraordinary morphological changes in valve morphology during the ontogeny of several species of the Australian ostracod genus *Bennelongia* (Crustacea, Ostracoda). European Journal of Taxonomy 36: 1–37.

Engel, M., H. Brückner, S. Fürstenberg, P. Frenzel, A. M. Konopczak, A. Scheffers, D. Kelletat, S. M. May, F. Schäbitz & G. Daut, 2013. A prehistoric tsunami induced long-lasting ecosystem changes on a semi-arid tropical island – the case of Boka Bartol (Bonaire, Leeward Antilles). Naturwissenschaften 100: 51–67.

Frenzel, P., C. Wrozyna, M. Xie, L. Zhu & A. Schwalb, 2010. Palaeo-water depth estimation for a 600-year record from Nam Co (Tibet) using an ostracod-based transfer function. Quaternary International 218: 157–165.

Frenzel, P., I. Schulze, A. Pint, I. Boomer & M. Feike, 2011. Salinity dependant morphological variation in *Cyprideis torosa*. Joannea Geologie und Paläontologie 11: 59–61.

Frenzel, P., I. Schulze & A. Pint, 2012. Noding of *Cyprideis torosa* valves (Ostracoda) – a proxy for salinity? New data from field observations and a long-term microcosm experiment. International Review of Hydrobiology 97: 314–329.

Frenzel, P., F. Günther, T. Kasper & K. Henkel, 2014. Paläoklimaforschung auf dem Dach der Welt. Biologie in Unserer Zeit 44: 108–115.

Hammer, Ø., D. A. T. Harper & P. D. Ryan, 2001. Past: paleontological statistics software package for education and data analysis. Palaeontologia Electronica 4: 9.

Hartmann, G., 1964. Das Problem der Buckelbildung auf Schalen von Ostracoden in ökologischer Sicht (mit Bemerkung zur Fauna des Trasimenischen Sees). Mitteilungen Hamburger zoologisches Museum und Institut 61(suppl.): 59–66.

Holmes, J. A., 1996. Ostracod faunal and microchemical evidence for middle Pleistocene sea-level change at Clacton-on-Sea (Essex, UK). In Keen, M. C. (ed.), Proceedings of the 2nd European Ostracodologists Meeting, Glasgow 1993. British Micropalaeontological Society, London: 135–140.

Hou, Y. T. & Y. X. Gou, 2007. Ostracod Fossils of China, vol. II, Cytheracea and Cytherellidae: 798 pp. (in Chinese with English summary).

Huang, B., H. Yang & K. You, 1982. Pliocene and Quaternary Ostracoda from southern and southwestern Xizang. In: Integrated Survey of Tibetan Plateau of Chinese Academy of Sciences, Palaeobiology of Xizang 4: 326–348 (in Chinese with English abstract).

Huang, B., L. Yang & Y. Fan, 1985. Ostracodes from surface deposits of recent lakes in Xizang. Acta Micropalaeontologia Sinica 2: 369–376. (in Chinese with English abstract).

Jochum, K. P., D. Scholz, B. Stoll, U. Weis, S. A. Wilson, Q. Yang, A. Schwalb, N. Börner, D. E. Jacob & M. O. Andreae, 2012. Accurate trace element analysis of speleothems and biogenic calcium carbonates by LA-ICP-MS. Chemical Geology 318–319: 31–44.

Karanovic, I., 2012. Recent Freshwater Ostracods of the World: Crustacea, Ostracoda, Podocopida. Springer, Berlin: 608 pp.

Keyser, D., 1990. Morphological changes and function of the inner lamella layer of podocopid Ostracoda. In Whatley, R. & C. Maybury (eds), Ostracoda and Global Events. Springer, Berlin: 633.

Keyser, D., 2005. Histological peculiarities of the noding process in *Cyprideis torosa* (Jones) (Crustacea, Ostracoda). Hydrobiologia 538: 95–106.

Keyser, D. & N. Aladin, 2004. Noding in *Cyprideis torosa* and its causes. Studia Quaternaria 21: 19–25.

Klie, W., 1938. Ostracoda, Muschelkrebse. Die Tierwelt Deutschlands und der angrenzenden Meeresteile nach ihren Merkmalen und nach ihrer Lebensweise. 34. Teil: Krebstiere oder Crustacea. Gustav Fischer, Jena: 230 pp.

Li, Y., Q. Zhang, B. Li & F. Liu, 1991. Late Pleistocene ostracoda from Bangong lake, Xizang and its palaeogeographic significance. Acta Micropalaeontologia Sinica 8: 57–64. [in Chinese with English abstract].

Linhart, J., W. Brauneis, W. Neubauer & D. L. Danielopol, 2006. Morphomatica, Computer Program Version 1.6 (http://palstrat.uni-graz.at/methods in ostracodology/methods in ostracodology_d.htm), Graz.

Mischke, S., U. Herzschuh, G. Massmann & C. Zhang, 2007. An ostracod-conductivity transfer function for Tibetan lakes. Journal of Paleolimnology 38: 509–524.

Mischke, S., B. Aichner, B. Diekmann, U. Herzschuh, B. Plessen, B. Wünnemann & C. Zhang, 2010. Ostracods and stable isotopes of a late glacial and Holocene lake record from the NE Tibetan Plateau. Chemical Geology 276: 95–103.

Pang, Q., 1985. On a new Ostracoda genus from Pleistocene in the pass of Kunlun Mountain, Qinghai-Xizang (Tibet) Plateau. Collection of Geology of the Qinghai-Xizang (Tibet) Plateau 16: 269–279. (in Chinese with English abstract).

Pang, Q., M. Zheng & W. Liu, 1985. The late Cenozoic Ostracoda of the Siling lake and Bangkog lake district in the Xizang (Tibet) and its stratigraphic significance. Contribution to the Geology of the Qinghai-Xizang (Tibet) Plateau 16: 260–266. (in Chinese with English abstract).

Peng, J., 1997. Ostracod assemblages and environmental changes during 13000–4500a BP in Peiku Co, Tibet. Acta Micropalaeontologica Sinica 14: 239–254. (in Chinese with English abstract).

Rohlf, F. J., 2004. TPSDig, Version 1.40. Department of Ecology and Evolution, State University of New York, Stony Brook.

Turpen, J. G. & R. W. Angell, 1971. Aspects of molting and calcification in the ostracod *Heterocypris*. The Biological Bulletin 140: 331–338.

Uffenorde, H. & G. Radtke, 2008. On noding in *Serrocytheridea* and *Hemicyprideis* (Cytherideinae) from the Early

Oligocene (Mainz Basin, SW Germany). Senckenbergiana lethaea 88: 77–92.

USGS, 2004. Shuttle Radar Topography Mission, 3 Arc Second scenes N28079–N33E091, Unfilled Unfinished 2.0, Global Land Cover Facility, University of Maryland, College Park, MD, February 2000.

Wrozyna, C., P. Frenzel, P. Steeb, L. Zhu & A. Schwalb, 2009a. Recent lacustrine Ostracoda and a first transfer function for palaeo-water depth estimation in Nam Co, southern Tibetan Plateau. Revista Española de Micropaleontología 41: 1–20.

Wrozyna, C., P. Frenzel, M. Xie, L. Zhu & A. Schwalb, 2009b. A taxonomical and ecological overview of recent and Holocene ostracodes of the Nam Co Region, Southern Tibet. Quaternary Sciences 29: 665–677.

Wrozyna, C., P. Frenzel, P. Steeb, R. van Geldern, A. Mackensen & A. Schwalb, 2010. Stable isotope and ostracode species assemblage evidence for lake level changes of Nam Co, southern Tibet, during the past 600 years. Quaternary International 212: 2–13.

Xia, J., E. Ito & D. R. Engstrom, 1997. Geochemistry of ostracode calcite: Part 1. An experimental determination of oxygene isotope fractionation. Geochimica et Cosmochimica Acta 61: 377–382.

Yang, Q., K. P. Jochum, B. Stoll, U. Weis, N. Börner, A. Schwalb, P. Frenzel, D. Scholz, S. Doberschütz, T. Haberzettl, G. Gleixner, R. Mäusbacher, L. Zhu & M. O. Andreae, 2014. Trace element variability in single ostracod valves as a proxy for hydrochemical change in Nam Co, central Tibet, during the Holocene. Palaeogeography, Palaeoclimatology, Palaeoecology 399: 225–235.

Yin, Y., W. Geiger & K. Martens, 1999. Effects of genotype and environment on phenotypic variability in *Limnocythere inopinata* (Crustacea, Ostracoda). Hydrobiologia 400: 85–144.

Zhu, L., P. Peng, M. Xie, J. Wang, P. Frenzel, C. Wrozyna & A. Schwalb, 2010. Ostracod-based reconstruction over the last 8,400 years of Nam Co Lake on the Tibetan plateau. Hydrobiologia 648: 157–174.